

Vanadium Oxide-Nitride Composites for Catalytic Oxidative C–C Bond Cleavage of Cyclohexanol into Lactones with Dioxygen

Chuhong Xiao,^[a, b] Zhongtian Du,^{*[a, b]} Shaojie Li,^[b] Yanbin Zhao,^[b] and Changhai Liang^{*[a, b]}

Selective catalytic oxidative C–C bond cleavage with dioxygen is useful and challenging to prepare oxygenated fine chemicals. Herein we fabricated vanadium oxide–nitride composites as catalysts via a facile thermal treatment process, and the surface composition could be tuned by the thermal treatment temperature, which could affect catalytic oxidation of cyclohexanol significantly. By using such a V–N–C composite prepared at 500 °C, cyclohexanol could be selectively oxidized with dioxygen into lactones including δ -valerolactone and γ -butyrolactone, rather than common dicarboxylic acids. Cyclohexanone and 2-cyclohexen-1-one were verified as two key intermediates. V^{3+} species in the form of vanadium nitride and vanadium (III) oxide were detected, and well dispersed on amorphous carbon with a low degree of graphitization. These findings will provide a reference for catalytic oxidative C–C bond cleavage with molecular oxygen under mild reaction conditions.

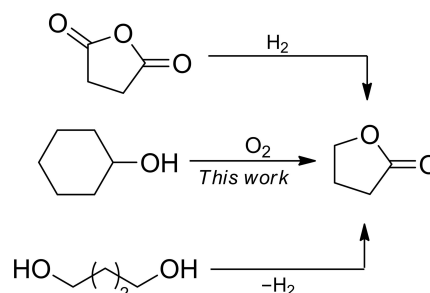
C–C bond is one of the most fundamental chemical bonds in organic molecules. Carbonyl groups could be generated through oxidative cleaving C–C bond, which would be useful in the fields such as synthesis of oxygenated fine chemicals, degradation of polymers and breakdown of lignocellulose etc.^[1–5] Due to high bond dissociation energies (BDEs) of C–C bonds (75–118 kcal/mol) as well as the inert molecular oxygen at the ground state,^[5] selective catalytic oxidative C–C bond cleavage with molecular oxygen under mild reaction conditions is rather attractive and challenging from both academic and industrial perspectives.^[6–8]

Lactones are important fine chemicals with a wide range of applications in industry, including pharmaceutical ingredients, cosmetics and polymer building blocks.^[9,10] *e.g.*, γ -butyrolactone (GBL) could be used as an intermediate in the manufacture of pyrrolidone derivatives, or as a solvent for polymers.^[9] Aliphatic polyesters prepared by ring-opening polymerization of δ -

valerolactone (DVL) have good mechanical properties, hydrolysability, and biocompatibility.^[10] Great efforts have been made to develop a variety of synthetic procedures for lactones. Three typical methods are often used for the synthesis of such cyclic intramolecular esters depending on different feedstocks (Scheme 1): (1) Baeyer–Villiger oxidation of ketones with peroxides,^[11] (2) oxidative lactonisation of diols,^[12] (3) selective reduction of carboxylic acids and their derivatives.^[13] The economic and environmental factors of these synthetic methods rely heavily on the starting materials and the related technical routes. It is rather attractive to develop novel methods for preparation of lactones, especially using inexpensive feedstocks.

The mixture of cyclohexanol/cyclohexanone (KA oil, 6×10^6 tons per year), is an important industrial raw material for the production of caprolactam and adipic acid.^[14] Oxidation of KA oil into adipic acid is usually performed with stoichiometric nitric acid in industry, which would generate a large amount of NO_x .^[14,15] Meanwhile catalytic oxidation of KA oil with molecular oxygen generally results in a mixture of dicarboxylic acids, which is unfavourable. However, few reports are disclosed for oxidation of cyclohexanol or cyclohexanone into intermediate oxygenates like lactones. The oxidative C–C bond cleavage is an effective approach to produce cyclic intramolecular esters by inserting oxygen atoms into cyclic compounds. We are interested in catalytic selective oxidation of cyclohexanol or cyclohexanone with molecular oxygen into lactones like γ -butyrolactone and δ -valerolactone, rather than dicarboxylic acids.

As a kind of abundant and non-precious metal, vanadium has a variety of chemistry, and is widely used in the field of catalytic oxidation.^[6,16,17] *e.g.*, vanadium phosphorus oxide (VPO) catalysts are efficient for *n*-butane oxidation into maleic anhydride in industry.^[18] For homogenous catalysis, oxovana-



Scheme 1. Several methods for the preparation of γ -butyrolactone (GBL).

[a] C. Xiao, Z. Du, Prof. C. Liang
State Key Laboratory of Fine Chemicals
Dalian University of Technology
Dalian, 116024 (P. R. China)
E-mail: duzhongtian@dlut.edu.cn
changhai@dlut.edu.cn

[b] C. Xiao, Z. Du, S. Li, Y. Zhao, Prof. C. Liang
School of Chemical Engineering
Dalian University of Technology
Panjin 124221 (P. R. China)

Supporting information for this article is available on the WWW under <https://doi.org/10.1002/cctc.202000288>

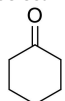
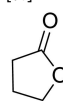
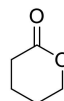
dium could also easily form complexes with heteroatom (*e.g.* O or N), and it is a typical strategy to regulate the catalytic performances of vanadium complexes by using different organic ligands.^[19–21] In previous reports, we also described unique activities of homogeneous vanadium catalysts for alcohol oxidation and oxidative C–C bond cleavage under mild reaction conditions.^[22–25] Recently, atomically dispersed metal–N–C materials have emerged as promising materials for various applications of interest such as energy storage, separation and catalysis.^[26–31] Research in this field has demonstrated that nitrogen doping is an effective way to tailor the properties of carbon and the electron density at the metal centers, which is analogous to the function of a ligand in homogeneous catalysis. We wonder the opportunities to modify the electronic environments and chemical structures of vanadium nanocatalysts, and tune their catalytic performances by introduction of nitrogen atoms. Herein we report V–N–C composites for catalytic oxidative C–C bond cleavage of cyclohexanol with molecular oxygen into lactones, and the surface structure of V–N–C catalysts prepared at different pyrolysis temperature varied greatly as well as the catalytic activity.

The fabrication process of the V–N–C catalysts is summarized as follows (Schematic illustration see Supporting Information, Scheme S1): Firstly, melamine was dispersed in hot water, and then NH_4VO_3 was added slowly under vigorous stirring (molar ratio of melamine/ NH_4VO_3 = 1:3). The solution was cooled at 0–5 °C, and the deposited blend was dried under vacuum at 100 °C. After grinding into a powder (V–N–C precursor), it was subjected to thermal treatment under a flow of nitrogen atmosphere at specifically regulated temperatures to afford the V–N–C catalysts. The materials calcined at different temperatures were denoted as V–N–C-*x* (*x*: thermal treatment temperature).

Initially, catalytic oxidation of cyclohexanol with molecular oxygen was carried out in acetonitrile (Table 1). As a secondary alcohol, cyclohexanol is generally resistant to oxidation with molecular oxygen. As expected, no significant oxidation took place without a catalyst (Table 1, entry 1). The materials calcined at different temperatures were used as the catalyst respectively. Only 2% conversion of cyclohexanol was observed when the

catalyst was prepared at 400 °C, and cyclohexanone was determined as the main product (Table 1, entry 2). Up to 89% of cyclohexanol was smoothly oxidized when V–N–C-500 was employed (Table 1, entry 3). Unexpectedly, oxidative C–C bond cleavage occurred. Only 23% selectivity of cyclohexanone was obtained, and up to 60% of lactones, including 40% of γ -butyrolactone and 20% of δ -valerolactone, were detected (Table 1, entry 3). Other products are mainly 2-cyclohexen-1-one, formic acid, cyclohexyl formate and carbon dioxide. Few reports have described the formation of lactones as main products via aerobic oxidation of cyclohexanol previously. Such a transformation would be rather attractive, as the selective oxidation could be tuned at lactones, rather than the common dicarboxylic acids. When V–N–C-600 was used as a catalyst, 95% of cyclohexanol could be oxidized, however, the total selectivity of lactones is only about 23%, and up to 73% selectivity of cyclohexanone was observed (Table 1, entry 4). Therefore, the thermal treatment temperature of V–N–C materials has great effects on the corresponding catalytic activities. Moreover, melamine and NH_4VO_3 was pyrolysis/calcined by a similar method at 500 °C, and the received materials (NH_4VO_3 -500 and melamine-500) were employed for catalytic oxidation. In contrast, low conversion of cyclohexanol was obtained respectively (Table 1, entries 5 and 6). Further, commercial V_2O_5 , NH_4VO_3 , and melamine was also used respectively in place of V–N–C-500 catalyst, however, the conversion of cyclohexanol was rather low under the same reaction conditions, and no lactones were observed (Table 1, entry 7). In a previous report, Tong and coworkers fabricated V–N–C composites via directly annealing the mixture of NH_4VO_3 and melamine as anode materials for lithium ion batteries.^[28] However, when V–N–C-mix-500 was prepared via a similar method and used for catalytic oxidation, low conversion of cyclohexanol was observed (Table 1, entry 8). All these experimental results suggest that the sample prepared at 500 °C exhibited unique catalytic activity for oxidative C–C bond fission of cyclohexanol, compared with V–N–C-400, V–N–C-600, and the starting materials. The structure of the V–N–C-500 catalyst will be discussed in the following paragraphs.

Table 1. Oxidation of cyclohexanol with dioxygen using different catalysts.^[a]

Entry	Catalyst	Conversion [%]	Selectivity of main products [%] ^[b]		
					
1	none	< 1	–	–	–
2	V–N–C-400	2	> 99	–	–
3	V–N–C-500	89	23	40	20
4	V–N–C-600	95	73	15	8
5 ^[c]	Melamine-500	2	> 99	–	–
6 ^[c]	NH_4VO_3 -500	2	> 99	–	–
7	V_2O_5	3	> 99	–	–
8 ^[d]	V–N–C-mix-500	2	> 99	–	–

[a] Reaction conditions: 5 mmol cyclohexanol, 5 wt% catalyst, 3 mL MeCN, 0.5 MPa O_2 , 120 °C, 8 h. [b] Other products, including 2-cyclohexen-1-one, cyclohexyl formate, formic acid and carbon dioxide, were detected. [c] Melamine or NH_4VO_3 was pyrolysed/calcined at 500 °C. [d] NH_4VO_3 and melamine was mixed mechanically before thermal treatment (molar ratio of melamine/ NH_4VO_3 = 1:3). For more details, see SI experimental section.

We further studied the reaction progress of cyclohexanol oxidation over V–N–C-500 catalyst (Figure 1). About 78% of cyclohexanol could smoothly be converted with 92% selectivity of cyclohexanone within 4 h, and only a few of lactones were detected. When the reaction time was prolonged to 6 h, the selectivity of lactones increased substantially, with the significant decrease of cyclohexanone. This observation suggests that cyclohexanone was probably an important intermediate during the oxidation of cyclohexanol into lactones. Within 8 h, 89% conversion of cyclohexanol could be obtained with 60% total selectivity of lactones, and the selectivity of cyclohexanone was also decreased to 23%. However, the conversion of cyclohexanol only increased slightly to about 90% after 10 h. It is notable that 1~2% of 2-cyclohexen-1-one always existed in the oxidation products from 4–10 h, which is probably related with the reaction pathway.

Now one of key issues is the structure and surface property of the V–N–C catalysts that related with catalytic oxidation. The catalysts calcined at different temperature (400, 500 and 600 °C) were analysed by X-ray diffractometer (XRD), as showed in Figure 2. Only a broad peak with low intensity located around 26° was observed from the XRD pattern of V–N–C-400. When the

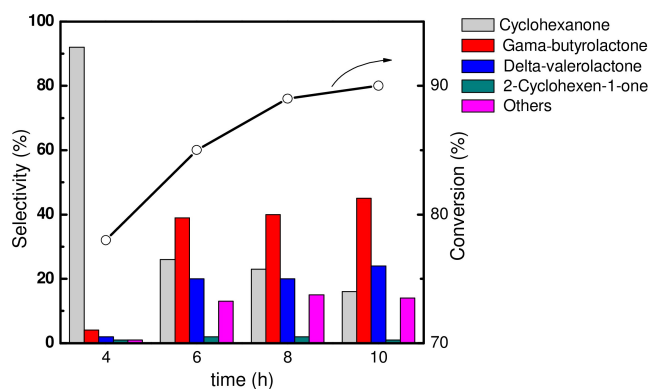


Figure 1. Reaction progress of cyclohexanol oxidation over the V–N–C-500 catalyst. Reaction conditions: 5 mmol cyclohexanol, 5 wt% catalyst, 3 mL MeCN, 0.5 MPa O₂, 120 °C.

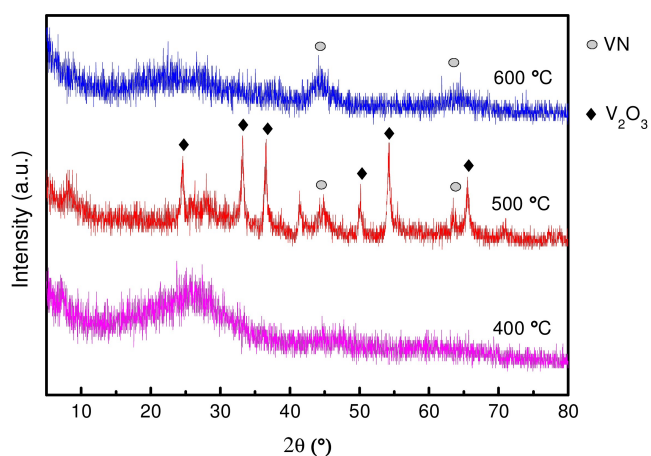


Figure 2. XRD patterns of V–N–C catalysts calcined at different temperature.

calcined temperature was 500 and 600 °C, the XRD patterns of received materials were quite different from that of V–N–C-400. The peaks around 26° were still broad and weak, which suggests the as-obtained materials possess amorphous carbon with a low degree of graphitization.^[32,33] V₂O₃ (PDF#76-0146) was detected from the pattern of V–N–C-500,^[34] which indicated that low-valence vanadium oxide appeared via the reduction reaction of NH₄VO₃. Weak peaks at 43.6 ° and 63.4° were also detected, which could be indexed to vanadium nitride (VN, PDF#35-0768).^[34,35] However, the peaks of VN in our work were much weaker than those in previous reports,^[34–36] demonstrating that part of vanadium oxides were transformed into VN with a low crystallinity. We further performed TG analysis to study the thermal treatment process of V–N–C-precursor (Supporting Information, Figure S3). The weight loss from 100 to 250 °C could be attributed to the absorbed water in surface and crystal water of the precursor. With the increase of temperature, the decomposition of NH₄VO₃ into V₂O₅ led to significant weight loss from 250~350 °C, as the melamine is stable before 354 °C. The decomposition of melamine as well as reduction of V₂O₅ took place between 350~600 °C, which could lead to the formation of VN and V_xO_y. When the temperature was further raised, only slight loss was observed. XRD and TG results clearly indicate that the precursor could be transformed into different V–N–C materials under different thermal treatment temperature. These changing structures should be related with the different catalytic activities for oxidative C–C bond cleavage.

The XPS studies were further performed to obtain more information about the surface composition of V–N–C-400, V–N–C-500 and V–N–C-600 (Figures 3, 4 and Figure S1). All the three materials have C, N, V, and O elements as depicted in the XPS survey spectra (Supporting Information, Figure S1, a). For the samples V–N–C-500 and V–N–C-600, the high-resolution of C 1s spectrum shows three fitting peaks (284.3, 286.0 and 288.6 eV, Figure S1, b in Supporting Information). The peak

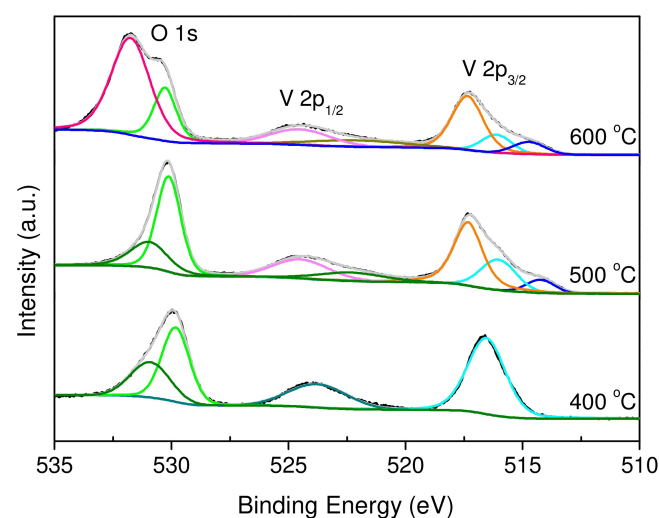


Figure 3. XPS spectra of O 1s and V 2p for the V–N–C-400, V–N–C-500 and V–N–C-600 catalysts.

around 284.3 eV could be ascribed to the doubly coordinated carbons, and the other two peaks of 286.0 and 288.6 eV can be assigned to C–N, and C=O bonds respectively.^[37,38] In contrast, for the sample prepared at 400 °C, the C 1s component of the XPS spectrum could only be divided into two main regions (284.4 and 287.9 eV). These results display the different existing form of carbon on the surface after pyrolysis at different temperature.

V 2p and O 1s components of the XPS spectra were usually put together for analysis because their binding energy is very close (Figure 3). The peaks from left to right correspond to O 1s, V 2p_{1/2}, and V 2p_{3/2}. The O 1s spectrum of V–N–C-400 and V–N–C-500 was divided into two main peaks centered at 529.9 and 531.0 eV, respectively. The peak at 529.9 eV suggests the existence of V–O component of vanadium oxides on the material surface.^[39,40] These results agree with XRD patterns mentioned above. Another peak at 531.8 eV in the V–N–C-600 sample could be attributed to the existence -OH groups formed in the process of heat treatment on the surface.^[40] These differences are reasonable, and consistent with the above XRD and C1s XPS analysis. As expected, the high-resolution V 2p_{3/2} XPS spectra also exhibit different oxidation states of vanadium (Figure 3). A peak at 516.6 eV was dominant for the V–N–C-400 sample, which could be ascribed to V⁴⁺ in the form of vanadium oxides.^[36] In contrast, the V2p_{3/2} spectra of the V–N–C-500 can obviously be divided into three peaks. The peaks at 514.3 eV could be attributed to V³⁺ species, which might be related with VN and V₂O₃, according to XRD and O 1s XPS analysis. Nevertheless, the bonding energy difference of vanadium species is very close, it is difficult to exactly distinguish the presence of vanadium oxynitride.^[39] Moreover, V⁴⁺ and V⁵⁺ species was also observed. The peaks at 516.2 eV were recognized as V⁴⁺ species, while the peaks at 517.4 eV were ascribed to V⁵⁺ species. Based on the analysis of the XPS spectra, we believe that V–N–C-500 and V–N–C-600 are mainly composed of vanadium oxide-nitride composites, together with amorphous carbon on the surface. Vanadium oxides and nitride with different oxidation states coexisted on the surface, and the distribution of vanadium with different oxidation states was shown in Figure S2 (Supporting Information). Approximately 10% of V³⁺, 29% of V⁴⁺, and 61% of V⁵⁺ were found in the sample of V–N–C-500, and 13% of V³⁺, 19% of V⁴⁺ and 67% of V⁵⁺ were detected for the sample of V–N–C-600. Meanwhile, nearly 100% V⁴⁺ was determined for V–N–C-400. As V–N–C-400 (V⁴⁺), NH₄VO₃-500 (V⁵⁺), and V₂O₅ (V⁵⁺) showed rather low catalytic activity (Table 1, entries 2, 6 and 7), the presence of V³⁺ species was most likely related with the enhanced catalytic activity for C–C bond cleavage, and the redox cycles of vanadium among different valence states are predictable during catalytic oxidation.

Additionally, the existing form of nitrogen was also quite different on the surface (Figure 4). For the N 1s line of V–N–C-500 and V–N–C-600, they were fitted with three peaks centered at 397.0, 399.2 and 401.8 eV by means of XPS peak differentiation-imitating analysis, corresponding to the characteristic of VN, pyrrolic, and graphitic nitrogen respectively.^[27,42] Approximately 20% of the nitrogen was bonded as pyrrolic nitrogen,

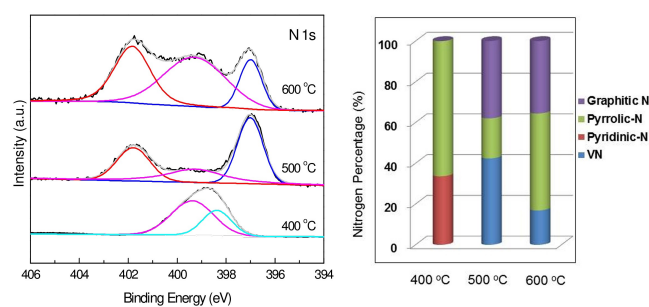


Figure 4. XPS spectra of N 1s (left) and types of nitrogen functionalities (right) for the V–N–C-400, V–N–C-500 and V–N–C-600 catalysts.

38% as graphitic nitrogen, and 42% as vanadium nitride (VN) for the sample of V–N–C-500, while 48% of the nitrogen was found as pyrrolic nitrogen, 35% as graphitic nitrogen, and 17% as vanadium nitride (VN) for that of V–N–C-600. In contrast, only two peaks at 398.4 and 399.4 eV were found for sample V–N–C-400, which were ascribed to pyridinic-N (34%) and pyrrolic-N (66%) respectively.^[27,38,43,44] Though the role of nitrogen species during catalytic oxidation is still unclear, the percentage of VN in the V–N–C-500 sample is highest among these materials, which meets the unique catalytic activity of V–N–C-500.

Raman spectroscopy is widely used to investigate the graphitic nature and concentration of defects in metal–N–C materials.^[27] We further performed Raman spectroscopy to detect more information about the V–N–C-500 sample (Supporting Information, Figure S4). The Raman peaks in the range of 100–1100 cm⁻¹ correspond to the characteristic peaks of vanadium oxides and VN, and the characteristic peaks at 140 and 281 cm⁻¹ are ascribed to acoustic band of VN, while that at 691 cm⁻¹ is related with optical band of VN.^[34,41] However, two bands centered at ca.1350 and 1560 cm⁻¹, which could be assigned to the disordered/defected carbon (D band) and graphitic sp² carbon (G band) respectively,^[27,38,45] are rather weak. These results demonstrate that the amorphous carbons predominate in the sample V–N–C-500 with a low degree of graphitization. VN and vanadium oxides coexist with such amorphous carbon composites with a low crystallinity, based on all the analysis depicted above.

The morphologies and microstructures of V–N–C composites were further examined. The scanning electron microscopy (SEM) images show that sheet-like morphology dominates, though the sample of V–N–C-500 does not have a specific shape (Supporting Information, Figure S5). The selected-area analysis of V–N–C-500 by the transmission electron microscopy (TEM) also indicates the presence of nano-sheets (Figure 5). Moreover, the corresponding EDS elemental mapping was also analysed. The green, orange, red, and yellow images stand for the distribution of V, N, C and O, respectively. The elements V, N, C and O were coexistent and homogeneously distributed throughout the whole V–N–C-500 composites. We believe that vanadium species (V_xO_y and VN) are well dispersed on the amorphous carbon successfully.

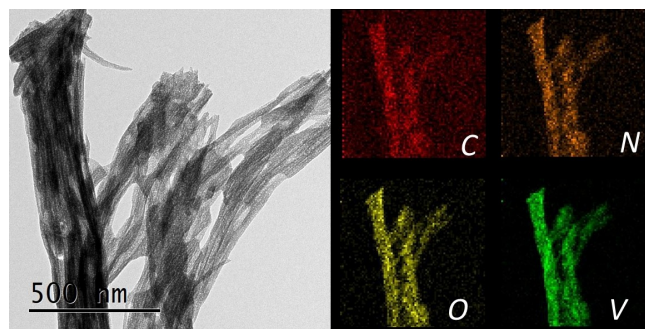


Figure 5. The TEM image and element mapping of V, N, C and O of the as-prepared V–N–C–500 catalyst.

Besides surface and structural property of catalysts, another important issue is the formation reaction pathway of lactones from cyclohexanol. Several control experiments were carried out over the V–N–C–500 catalyst (Supporting Information, Table S4). When the reaction of cyclohexanol was performed under a nitrogen atmosphere, only 4% conversion of cyclohexanol was observed with 8 h, and no lactones were detected. Thus, the dehydrogenation reaction under an inert environment is not dominant, and molecular oxygen is indispensable. Catalytic oxidation of cyclohexanol was also tested in the presence of 5 mol% free radical inhibitors including 2,6-di-tert-butyl-*p*-cresol (BHT) and 2,2,6,6-tetramethyl-1-piperidinyloxy (TEMPO). Unexpectedly, 90% and 94% conversion of cyclohexanol could still be obtained with 48% and 25% selectivity of total lactones within 8 h respectively. These results suggest that free radical chain reactions did not predominate during oxidation of cyclohexanol into lactones. As described above (Figure 1), the reaction progress profile showed that cyclohexanone was the major product within 4 h, and decreased significantly when the reaction time was prolonged. As expected, when cyclohexanone was directly subjected to oxidation (Supporting Information, Scheme S2), it was smoothly converted into γ -butyrolactone and δ -valerolactone with 99% conversion in 8 h, and the total selectivity of lactones is up to 79%. Thus, cyclohexanone was undoubtedly one of key intermediates during the formation of lactones. Moreover, 2-cyclohexen-1-one was always detected in the oxidation products, though the concentration was always rather low. We subsequently performed the direct oxidation of 2-cyclohexen-1-one under the same reaction conditions above. To our delight, 76% selectivity of γ -butyrolactone was observed with 19% conversion of 2-cyclohexen-1-one (Supporting Information, Scheme S2). Further we carried out catalytic oxidation of γ -butyrolactone and δ -valerolactone under the same reaction conditions, and no further oxidation was observed, which indicated that γ -butyrolactone and δ -valerolactone could remain stable under the oxidative reaction conditions.

Based on the above results, we reasoned a proposed reaction pathway from cyclohexanol to lactones over V–N–C catalysts (Supporting Information, Scheme S3). Firstly, cyclohexanol was oxidized into cyclohexanone, and then further

oxidation of cyclohexanone might afford 2-hydroxy-1-cyclohexanone.^[14,15,46] Vanadium-catalyzed C–C bond cleavage of 2-hydroxy-1-cyclohexanone into dicarboxylic acid with molecular oxygen was known in previous reports.^[47,48] It is reasonable that selective oxidation of 2-hydroxy-1-cyclohexanone into lactones via C–C bond cleavage occurred over V–N–C catalysts, which could afford δ -valerolactone. Meanwhile 2-cyclohexen-1-one was also produced via dehydration, and then oxidized into γ -butyrolactone. These lactones are resistant to further oxidation.

Finally, the reusability of the V–N–C composites was investigated for catalytic oxidation of cyclohexanol with molecular oxygen. However, direct reuse of the V–N–C–500 catalyst exhibited much lower catalytic activity under the same reaction conditions. Only 17% conversion of cyclohexanol was obtained within 8 h, and cyclohexanone was the only product. The catalyst after use became dark green, while the fresh is black. Only a broad and weak peak around 25 °C could be observed from the XRD pattern of the V–N–C–500 after use (Supporting Information, Figure S6), which is quite different from that before use. There are several possible aspects that caused the activity loss for V–N–C materials in liquid phase oxidation. When molecular oxygen is used as an oxidant, water was gradually released as a byproduct. We previously observed the deactivation of some vanadium catalytic systems by water.^[22,49] Furthermore, formic acid was also formed due to oxidative C–C bond cleavage (Supporting Information, Figure S7), and such an acidic environment would cause destruction of vanadium oxides,^[50] and neutralize basic nitrogen-containing species, which could result in a significant change of vanadium active sites and the corresponding catalytic activity.

In summary, vanadium oxide–nitride composites in the form of nano-sheets were fabricated via a facile thermal treatment process. Cyclohexanol could be selectively oxidized with molecular oxygen into valuable lactones including δ -valerolactone and γ -butyrolactone, rather than dicarboxylic acids. The thermal treatment temperature could alter the surface and structural property of these V–N–C composites significantly, and affect the catalytic activities consequently. Over the V–N–C–500 catalyst, 89% conversion of cyclohexanol could easily be obtained with a 60% total selectivity of lactones at 120 °C within 8 h. Cyclohexanone and 2-cyclohexen-1-one were verified as two key intermediates. V^{3+} species in the form of vanadium nitride and vanadium (III) oxide were well dispersed on amorphous carbon with a low degree of graphitization, which was most likely related with the enhanced catalytic activity for oxidative C–C bond cleavage. These results will provide researchers with new ideas for catalytic oxidative C–C bond cleavage, and would be also useful in the other fields such as breakdown of lignocellulose and degradation of polymers.

Acknowledgements

This work was supported by the National Natural Science Foundation of China (21473184), the Fundamental Research

Funds for the Central Universities (DUT15RC(3)094), and the Natural Science Foundation of Liaoning Province (2019-MS-047).

Conflict of Interest

The authors declare no conflict of interest.

Keywords: Lactones · Oxidation · Heterogeneous catalysis · Vanadium · C–C bond cleavage

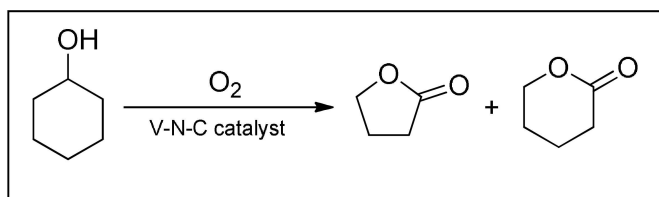
- [1] V. Escande, C. H. Lam, P. Coish, P. T. Anastas, *Angew. Chem. Int. Ed.* **2017**, *56*, 9561–9565; *Angew. Chem.* **2017**, *129*, 9689–9693.
- [2] H. Luo, L. Wang, G. Li, S. Shang, Y. Lv, J. Niu, S. Gao, *ACS Sustainable Chem. Eng.* **2018**, *6*, 14188–14196.
- [3] M. Huang, X. Li, M. Zou, S. Song, C. Tang, Y. Yuan, N. Jiao, *J. Am. Chem. Soc.* **2014**, *136*, 14858–14865.
- [4] S. K. Hanson, R. Wu, L. A. P. Silks, *Angew. Chem. Int. Ed.* **2012**, *51*, 3410–3413; *Angew. Chem.* **2012**, *124*, 3466–3469.
- [5] L. Shuai, J. Sitison, S. Sadula, J. Ding, M. C. Thies, B. Saha, *ACS Catal.* **2018**, *8*, 6507–6512.
- [6] E. Amadio, R. Di Lorenzo, C. Zonta, G. Licini, *Coord. Chem. Rev.* **2015**, *301*, 147–162.
- [7] W. Schwarz, J. Schossig, R. Roszbacher, H. Höke, *Butyrolactone in Ullmann's Encyclopedia of Industrial Chemistry* (7th Edition), Wiley-VCH, Weinheim, **2011**.
- [8] K. Makiguchi, T. Satoh, T. Kakuchi, *Macromolecules* **2011**, *44*, 1999–2005.
- [9] A. Corma, L. T. Nemeth, M. Renz, S. Valencia, *Nature* **2001**, *412*, 423–425.
- [10] T. Mitsudome, A. Noujima, T. Mizugaki, K. Jitsukawa, K. Kaneda, *Green Chem.* **2009**, *11*, 793–797.
- [11] M. Selva, M. Gottardo, A. Perosa, *ACS Sustainable Chem. Eng.* **2013**, *1*, 180–189.
- [12] S. Van de Vyver, Y. Roman-Leshkov, *Catal. Sci. Technol.* **2013**, *3*, 1465–1479.
- [13] J. C. J. Bart, S. Cavallaro, *Ind. Eng. Chem. Res.* **2015**, *54*, 1–46.
- [14] M. Kiriwara, *Coord. Chem. Rev.* **2011**, *255*, 2281–2302.
- [15] R. R. Langeslay, D. M. Kaphan, C. L. Marshall, P. C. Stair, A. P. Sattelberger, M. Delferro, *Chem. Rev.* **2019**, *119*, 2128–2191.
- [16] F. Cavani, J. H. Teles, *ChemSusChem* **2009**, *2*, 508–534.
- [17] A. Butler, M. J. Clague, G. E. Meister, *Chem. Rev.* **1994**, *94*, 625–638.
- [18] M. Sutradhar, L. M. D. R. S. Martins, M. F. C. G. da Silva, A. J. L. Pombeiro, *Coord. Chem. Rev.* **2015**, *301*, 200–239.
- [19] S. K. Hanson, R. Wu, L. A. P. Silks, *Org. Lett.* **2011**, *13*, 1908–1911.
- [20] Z. Du, J. Liu, T. Lu, Y. Ma, J. Xu, *Sci. China Chem.* **2015**, *58*, 114–122.
- [21] Y. Ma, Z. Du, J. Liu, F. Xia, J. Xu, *Green Chem.* **2015**, *17*, 4968–4973.
- [22] J. Liu, Z. Du, Y. Yang, T. Lu, F. Lu, J. Xu, *ChemSusChem* **2012**, *5*, 2151–2154.
- [23] Z. Du, J. Ma, F. Wang, J. Liu, J. Xu, *Green Chem.* **2011**, *13*, 554–557.
- [24] D. Zhao, K. Sun, W.-C. Cheong, L. Zheng, C. Zhang, S. Liu, X. Cao, K. Wu, Y. Pan, Z. Zhuang, B. Hu, D. Wang, Q. Peng, C. Chen, Y. Li, *Angew. Chem. Int. Ed.* In press, DOI: 10.1002/anie.201908760.
- [25] L. He, F. Weniger, H. Neumann, M. Beller, *Angew. Chem. Int. Ed.* **2016**, *55*, 12582–12594; *Angew. Chem.* **2016**, *128*, 12770–12783.
- [26] B. Long, M.-S. Balogun, L. Luo, Y. Luo, W. Qiu, S. Song, L. Zhang, Y. Tong, *Small* **2017**, *13*, 1702081.
- [27] M. Li, F. Xu, H. Li, Y. Wang, *Catal. Sci. Technol.* **2016**, *6*, 3670–3693.
- [28] X.-H. Li, M. Antonietti, *Chem. Soc. Rev.* **2013**, *42*, 6593–6604.
- [29] Y. Pan, Y. Chen, K. Wu, Z. Chen, S. Liu, X. Cao, W.-C. Cheong, T. Meng, J. Luo, L. Zheng, C. Liu, D. Wang, Q. Peng, J. Li, C. Chen, *Nat. Commun.* **2019**, *10*, 4290.
- [30] J. Liu, F. Li, W. Liu, X. Li, *Inorg. Chem. Front.* **2019**, *6*, 164–171.
- [31] J. Peng, N. Chen, R. He, Z. Wang, S. Dai, X. Jin, *Angew. Chem. Int. Ed.* **2017**, *56*, 1751–1755; *Angew. Chem.* **2017**, *129*, 1777–1781.
- [32] M. Wu, H. Guo, Y.-n. Lin, K. Wu, T. Ma, A. Hagfeldt, *J. Phys. Chem. C* **2014**, *118*, 12625–12631.
- [33] F. Cheng, C. He, D. Shu, H. Chen, J. Zhang, S. Tang, D. E. Finlow, *Mater. Chem. Phys.* **2011**, *131*, 268–273.
- [34] A. M. Glushenkov, D. Hulicova-Jurcakova, D. Llewellyn, G. Q. Lu, Y. Chen, *Chem. Mater.* **2010**, *22*, 914–921.
- [35] Y. Wu, F. Ran, *J. Power Sources* **2017**, *344*, 1–10.
- [36] W. Zhang, P. Oulego, T. K. Slot, G. Rothenberg, N. R. Shiju, *ChemCatChem* **2019**, *11*, 3381–3387.
- [37] E. F. de Souza, C. A. Chagas, T. C. Ramalho, V. T. da Silva, D. L. M. Aguiar, R. San Gil, R. B. de Alencastro, *J. Phys. Chem. C* **2013**, *117*, 25659–25668.
- [38] Y. Yang, L. Zhao, K. Shen, Y. Liu, X. Zhao, Y. Wu, Y. Wang, F. Ran, *J. Power Sources* **2016**, *333*, 61–71.
- [39] C. M. Ghimbeu, E. Raymundo-Pinero, P. Fioux, F. Beguin, C. Vix-Guterl, *J. Mater. Chem.* **2011**, *21*, 13268–13275.
- [40] T. Lin, I. W. Chen, F. Liu, C. Yang, H. Bi, F. Xu, F. Huang, *Science* **2015**, *350*, 1508–1513.
- [41] R. Arrigo, M. Haevecker, R. Schloegl, D. S. Su, *Chem. Commun.* **2008**, 4891–4893.
- [42] X. Wang, C.-G. Liu, D. Neff, P. F. Fulvio, R. T. Mayes, A. Zhamu, Q. Fang, G. Chen, H. M. Meyer, B. Z. Jang, S. Dai, *J. Mater. Chem. A* **2013**, *1*, 7920–7926.
- [43] L. Qie, W.-M. Chen, Z.-H. Wang, Q.-G. Shao, X. Li, L.-X. Yuan, X.-L. Hu, W.-X. Zhang, Y.-H. Huang, *Adv. Mater.* **2012**, *24*, 2047–2050.
- [44] F. Cavani, L. Ferroni, A. Frattini, C. Lucarelli, A. Mazzini, K. Raabova, S. Alini, P. Accorinti, P. Babini, *Appl. Catal. A* **2011**, *391*, 118–124.
- [45] M. Vennat, P. Herson, J. M. Bregeault, G. B. Shul'pin, *Eur. J. Inorg. Chem.* **2003**, 908–917.
- [46] L. El Aakel, F. Launay, A. Atlamsani, J. M. Bregeault, *Chem. Commun.* **2001**, 2218–2219.
- [47] Z. Du, J. Ma, H. Ma, J. Gao, J. Xu, *Green Chem.* **2010**, *12*, 590–592.
- [48] D. Rehder, *Bioinorganic Vanadium Chemistry*. John Wiley & Sons, Chichester, **2008**, 13–26.

Manuscript received: February 17, 2020

Revised manuscript received: March 28, 2020

Version of record online: ■■■, ■■■■

COMMUNICATIONS



V–N–C catalysts were prepared via a thermal treatment process for catalytic oxidative C–C bond cleavage with molecular oxygen. Cyclohexanol was selectively oxidized with dioxygen into lactones including δ-valerolactone and γ-butyrolactone,

rather than common dicarboxylic acids. Cyclohexanone and 2-cyclohexen-1-one were verified as two key intermediates, and vanadium nitride and vanadium (III) oxide were detected on the surface of V–N–C-500.

C. Xiao, Z. Du, S. Li, Y. Zhao, Prof. C. Liang**

1 – 7

Vanadium Oxide-Nitride Composites for Catalytic Oxidative C–C Bond Cleavage of Cyclohexanol into Lactones with Dioxygen

